THE ASTROPHYSICAL JOURNAL, 542:978–988, 2000 October 20

TWO K GIANTS WITH SUPERMETEORITIC LITHIUM ABUNDANCES: HDE 233517 AND HD 9746

SUCHITRA C. BALACHANDRAN[1]
University of Maryland, Department of Astronomy, College Park, MD 20742; suchitra@astro.umd.edu
FRANCIS C. FEKEL[1] AND GREGORY W. HENRY
Center of Excellence in Information Systems, Tennessee State University, 330 10th Avenue North, Nashville, TN 37203; fekel@evans.tsuniv.edu, henry@schwab.tsuniv.edu
AND
HAN UITENBROEK
Harvard-Smithsonian Center for Astrophysics, 60 Garden Street, Cambridge, MA 02138; huitenbroek@cfa.harvard.edu
Received 2000 April 3; accepted 2000 June 2

ABSTRACT

Two unusual Li-rich K giants, HDE 233517 and HD 9746, have been studied. Optical spectroscopy and photometry have been obtained to determine the fundamental parameters of HDE 233517, a single K2 III with an extremely large infrared excess. The spectra yield $T_{\rm eff} = 4475$ K, $\log g = 2.25$, [Fe/H] $= -0.37$, $v \sin i = 17.6$ km s^{-1}, and a non-LTE $\log \epsilon(^7{\rm Li}) = 4.22$. Photometric observations reveal low-amplitude light variability with a period of 47.9 days. Combined with other parameters, this results in a minimum radius of 16.7 $R_\odot$ and minimum distance of 617 pc. Comparison of spectra obtained in 1994 and 1996 show profile variations in Hα and the Na D lines indicative of changing mass loss. Optical spectra of HD 9746, a chromospherically active giant, were analyzed. The $T_{\rm eff} = 4400$ K and revised *Hipparcos*-based gravity of $\log g = 2.30$ lead to a non-LTE $\log \epsilon(^7{\rm Li}) = 3.75$. The Li abundances in both stars are supermeteoritic. By the inclusion and exclusion of ^{6}Li in the syntheses, we show that consistent ^{7}Li abundances are obtained only when ^{6}Li is absent in the synthetic fit. This provides evidence for fresh ^{7}Li production and excludes both preservation of primordial Li and planetary accretion as viable scenarios for the formation of Li-rich giants. Both stars lie in close proximity to the red giant luminosity bump supporting the hypothesis that ^{7}Li production is caused by the same mixing mechanism that later results in CN processing and lowers the ^{12}C/^{13}C ratio to nonstandard values.

Subject headings: nuclear reactions, nucleosynthesis, abundances — stars: abundances — stars: individual (HD 9746, HDE 233517) — stars: late-type

1. INTRODUCTION

Walker & Wolstencroft (1988) listed HDE 233517 as one of several stars with infrared characteristics similar to Vega, indicating the presence of a cool dust disk. It was first investigated extensively by Skinner et al. (1995), who obtained near-infrared photometry, mid-infrared spectra, and a mid-infrared image. The agreement of a K dwarf surface-flux model with their observations and the evidence of a resolved dust disk around the star having oxygen-rich and carbon-rich grains of various sizes led them to argue that HDE 233517 is a young, chromospherically active K dwarf rather than a giant. In fact, Skinner et al. (1995) concluded that if HDE 233517 is a giant, it is "possibly the most extraordinary post–main-sequence star so far discovered." Miroshnichenko, Bergner, & Kuratov (1996) obtained optical and near-infrared photometry during a 12 day interval but were unable to detect any photometric variations. From an analysis of its color indices, they concluded that HDE 233517 is a late K dwarf. Fekel et al.'s (1996) follow-up optical spectroscopy produced additional results, some of which were at odds with previous conclusions. While they showed that the star has modest Ca II H and K emission, indicative of chromospheric activity, they classified it not as a dwarf but as a K2 III. They also discovered that HDE 233517 is rapidly rotating, having $v \sin i = 15$ km s^{-1}, but was likely single, showing no significant velocity variations. They found an extremely large log Li abundance of 3.3 and an Hα profile suggesting a stellar wind and mass loss. They argued that HDE 233517 is a post–main-sequence giant putting it in the unusual class of Li-rich giants (Wallerstein & Sneden 1982; Brown et al. 1989; Gratton & D'Antona 1989; Pilachowski, Sneden, & Hudek 1990; Fekel & Balachandran 1993; de la Reza & da Silva 1995).

To examine further the conclusions of Fekel et al. (1996) about this most unusual post–main-sequence giant, we have searched for photometric evidence of rotational modulation; obtained additional radial velocities; remeasured its $v \sin i$ value; and determined its spectroscopic temperature, gravity, and Fe abundances as well as an improved value of its Li abundance from the resonance and excited Li I lines via LTE and non-LTE analyses. We have also compared profiles of the strong Na D, Hα, K I, and Li I lines in two spectra of HDE 233517 taken 2 yr apart and find startling differences in some lines.

These results led to a reanalysis of the Li abundance of HD 9746, another chromospherically active Li-rich K giant (Brown et al. 1989; Fekel & Balachandran 1993).

2. NEW OBSERVATIONS AND REDUCTIONS

2.1. *Photometry*

Beginning with the 1994–1995 season, we placed HDE 233517 on the observing menu of the T3 0.4 m automatic photoelectric telescope (APT) at Fairborn Observatory. The star was observed through Johnson B and V filters in

[1] Visiting Astronomer, Kitt Peak National Observatory, National Optical Astronomy Observatories, operated by the Association of Universities for Research in Astronomy, Inc., under contract to the National Science Foundation.

our standard group sequence for differential photometry: K, S, C, V, C, V, C, V, C, S, K, where K is a check star (HD 69682: $V = 6.50$, $B-V = 0.29$, F0 V), S is a sky position, C is the comparison star (HD 70295: $V = 8.8$, $B-V = 0.7$, K0), and V is HDE 233517. A focal-plane diaphragm with a 40″ diameter was employed to exclude the light of 9.0 mag HD 233520, located only 55″ from HDE 233517.

The average of the $V-C$ and $K-C$ differential magnitudes within each group sequence was formed and treated as single observation thereafter. We used nightly extinction coefficients and yearly mean transformation coefficients, all determined from nightly observations of standard stars, to correct the differential magnitudes for extinction and transform them to the Johnson UBV system. The external precision of a single observation, defined as the standard deviation of a single group mean from the seasonal mean magnitude, is typically 0.003–0.004 mag for constant pairs of stars (Henry 1995a). Further details about the telescope, precision photometer, automated data acquisition, and reduction and precision of the observations can be found in Henry (1995a, 1995b, 1996).

2.2. *Spectroscopy*

High-resolution echelle spectra of HDE 233517 were acquired at the 4 m Kitt Peak National Observatory (KPNO) telescope with the Cassegrain echelle spectrograph on 1994 November 17 and 1996 November 24. The former was a single 15 minute exposure, the latter consisted of two spectra of 10 minutes each. The spectrograph set up in the two cases was identical. The long-focus red camera was used with the 58.5 echelle grating and the 226-1 cross-disperser. A red GG-495 filter was used to cut off short wavelengths. The spectral resolution was $R = 35{,}000$.

The spectra were reduced with standard IRAF routines. The bias level was subtracted, the spectra were flat-fielded, cosmic rays were removed, and the individual orders were extracted. The wavelength scale was established with a Th-Ar comparison spectrum. The 1994 spectrum has 20 orders extending from 5550 to 8750 Å. The 1996 spectrum has 23 orders extending from 5050 to 8300 Å.

Between 1996 October and 1999 October, four additional spectra of HDE 233517 were obtained with the KPNO coudé feed telescope and coudé spectrograph and a TI CCD detector. The observations are centered at a wavelength of 6430 Å and have a wavelength range of about 80 Å and a resolution of 0.21 Å. Bias subtraction, flat-field division, wavelength calibration, and continuum rectification were performed on the raw spectra with the programs in IRAF. Th-Ar comparison spectra were obtained each night at intervals of 1–2 hr to ensure an accurate wavelength calibration.

With the coudé feed telescope plus the same spectrograph and detector combination used for the observations of HDE 233517, one spectrum of HD 9746 in the 6103.6 Å Li I excited-line region was obtained on 1997 July 4 with a resolution of 0.21 Å and a signal-to-noise ratio of 250:1.

3. HDE 233517: ANALYSIS AND RESULTS

3.1. *Photometry*

A total of 338 group observations were acquired by the APT during four observing seasons. Comparison of the $V-C$ and $K-C$ differential magnitudes reveals that both HDE 233517 and the K0 comparison star HD 70295 are new, low-amplitude variables. Little is known about HD 70295 other than its K0 spectral classification and low proper motion. Our $K-C$ differential magnitudes suggest a period of about 138 ± 5 days and an amplitude between 0.01 and 0.02 mag for HD 70295. Consequently, we formed $V-K$ differential magnitudes to analyze the light variations of HDE 233517 against the constant check star. Because the 65 observations in the second (1995–1996) observing season, extending from JD 2,449,984 to JD 2,450,219, showed the most coherent light variation, we restrict the present analysis to that season. The same periodicity was present in the first observing season, while no significant periodicity was detectable in the third and fourth seasons because the photometric amplitude became too small.

Separate periodogram analyses of the B and V observations from the second season gave periods of 48.5 ± 0.8 and 47.0 ± 1.0 days, respectively, for HDE 233517. The weighted mean of these two determinations is 47.9 ± 0.6 days (Table 1). Figure 1 shows the V observations plotted modulo the 47.9 day period. A least-squares sine fit to the data in Figure 1 gives a full amplitude of 0.020 ± 0.003 mag.

3.2. *Radial Velocity*

Radial velocities relative to the IAU radial velocity standards HR 1283 or HR 3145 were determined from our four coudé spectra with the IRAF cross-correlation program FXCOR (Fitzpatrick 1993). Velocities of the standards were adopted from Scarfe, Batten, & Fletcher (1990). Combined

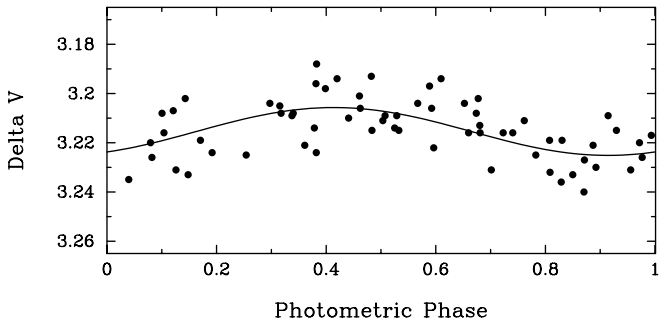

FIG. 1.—Johnson V APT observations of HDE 233517 from the 1995–1996 observing season plotted against the 47.9 day photometric period. The continuous curve is the least-squares sine fit to the observations and has an amplitude of 0.020 ± 0.003 mag.

TABLE 1

BASIC PROPERTIES OF HDE 233517 AND HD 9746

Parameter	HDE 233517	HD 9746
V (mag)	9.72[a]	5.92[b]
$B-V$ (mag)	1.32[a]	1.21[b]
Spectral type	K2 III[a]	K1 III[c]
V_r (km s^{-1})	46.2 ± 0.1[d]	-42.6[c]
$v \sin i$ (km s^{-1})	17.6 ± 1.0[d]	9.0 ± 1.0[e]
P_{rot} (days)	47.9 ± 0.6[d]	76.0 ± 1.3[f]

[a] Fekel et al. 1996.
[b] Nicolet 1978.
[c] Fekel & Balachandran 1993.
[d] This paper.
[e] Fekel 1997.
[f] Strassmeier & Hall 1988.

with the eight velocities obtained by Fekel et al. (1996), the four new velocities extend the date range to 5.5 yr, from 1994 April to 1999 October (Table 2). The mean velocity is 46.2 ± 0.1 km s^{-1} (Table 1), and there continues to be no evidence of velocity variability. Thus, our additional velocities support the conclusion of Fekel et al. (1996) that HDE 233517 is a single star.

3.3. *Projected Rotational Velocity*

The v sin i value of HDE 233517 was determined by following the procedure of Fekel (1997). For each of the seven coudé feed spectra obtained at 6430 Å (Table 2), the FWHM of several moderate strength lines was measured and the results averaged. An instrumental broadening of 0.21 Å was removed from the measured mean broadening by taking the square root of the difference between the squares of the stellar- and comparison-line measurements, resulting in the intrinsic stellar broadening. Next Fekel's (1997) calibration polynomial was used to convert this broadening in angstroms into a total line broadening in km s^{-1}. Finally, the macroturbulence, assumed to be 3 km s^{-1}, was removed by taking the square root of the difference of the squares, resulting in the projected rotational velocity. The mean projected rotational velocity is 17.6 km s^{-1} with an estimated uncertainty of 1.0 km s^{-1}. Listed in Table 1, this value supersedes the one determined by Fekel et al. (1996).

3.4. *Line Profiles*

Fekel et al. (1996) commented on the unusual Hα line profile of HDE 233517. They compared an Hα region spectrum of HDE 233517 to the same region in the rotationally broadened spectrum of α Ari (K2 III) and found that while all other lines matched well, the Hα line of HDE 233517 was far broader than that of α Ari. The Hα feature of HDE 233517 was also asymmetric with a blueshifted core and a modest blueshifted emission peak. Fekel et al. (1996) noted that the line profile was similar to that of the supergiant ϵ Gem (Mallik 1993; Eaton 1995). The line shape of the latter is attributed to an expanding chromospheric wind with mass outflow in the range of 10^{-8} to $10^{-9}\ M_\odot$ yr^{-1}.

Since the dispersions of the 1994 and 1996 echelle spectra are identical, a search for possible temporal variations in line profiles is greatly simplified. A comparison of the Hα lines in the two spectra (Fig. 2*a*) shows that the profiles are significantly different. The 1996 spectrum has a deeper and broader Hα feature compared to the 1994 spectrum. The blue wing rising above the continuum in the 1994 spectrum is absent in the 1996 spectrum. In addition, although both profiles are clearly asymmetric, the sharp change in the profile redward of line minimum in the 1994 spectrum is not seen in the 1996 spectrum. Figure 2*a* also shows the difference between the 1994 and 1996 spectra. Two components are seen in the difference, with additional absorption centered at roughly -32 and $+36$ km s^{-1} with respect to the central wavelength of the Hα line at 6562.81 Å, with the redward component being the stronger of the two.

TABLE 2

RADIAL VELOCITIES OF HDE 233517

Date (HJD − 2,400,000)	Radial Velocity (km s^{-1})	Wavelength Region (Å)
49,444.656	46.5	5800–9400
49,622.012	46.0	6430
49,675.009	46.1	6565
49,676.994	46.4	6430
49,678.027	46.2	6695
49,833.718	46.4	6430
49,836.737	47.2	3950
49,838.660	46.2	3950
50,366.023	45.6	6430
50,367.018	45.6	6430
50,833.853	46.1	6430
51,476.026	46.2	6430

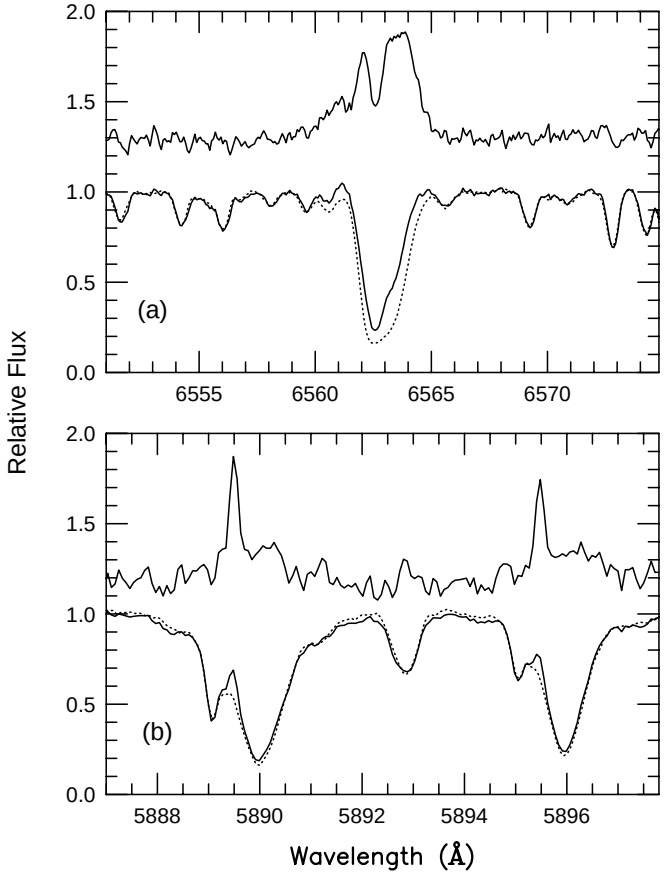

FIG. 2.—(*a*) Hα and (*b*) Na D lines from the 1994 (*solid line*) and 1996 (*dotted line*) spectra of HDE 233517 are compared. Each difference spectrum is shown multiplied by a scale factor and vertically displaced.

The Na D lines of our 1994 and 1996 spectra are shown in Figure 2*b*. Each photospheric Na D line is flanked on the blueward side by an additional absorption line. The satellite features are displaced roughly -46.5 km s^{-1} from the central wavelengths of the photospheric Na D lines. Fekel et al. (1996) noted that the blueshifted absorption lines are narrow, their velocities closely correspond to the local standard of rest, and their equivalent widths are consistent with a distance of a few hundred parsecs as inferred from interstellar medium (ISM) absorption (Hobbs 1974). For those reasons they concluded that the sharp features are of interstellar rather than stellar origin. We concur and further note that the sharp lines cancel out fully when the 1994 and 1996 spectra are differenced (Fig. 2*b*), as may be expected for interstellar lines. However, just as in the case of Hα, two components are seen in the Na D differenced spectrum: one is at roughly -24 to -25 km s^{-1} from the nominal line

center, similar to that seen in Hα, and the other is broader and displaced only about $+10$ km s^{-1} from the nominal central wavelength.

No differences in line profiles are seen in any other features. In particular, we carefully examined the Li I resonance line at 6707.8 Å and the K I resonance line at 7699.0 Å.

3.5. *Atmospheric Parameters*

The effective temperature ($T_{\rm eff}$), gravity ($\log g$), and microturbulent velocity (ξ) of HDE 233517, all parameters required for an abundance analysis, were determined spectroscopically. The equivalent widths of 49 Fe I and seven Fe II lines between 6000 and 7800 Å were measured in the 1994 spectrum. Solar oscillator strengths were derived for these lines by measuring their equivalent widths in the digital version of the Solar Flux Atlas (Kurucz et al. 1984) and requiring them to produce the solar Fe abundance of $\log \epsilon({\rm Fe}) = 7.52$ with the Kurucz solar model ($T_{\rm eff} = 5770$ K, $\log g = 4.4$, no convective overshoot). A recently modified version of the standard program MOOG (Sneden 1973) was used in the abundance analysis. The effective temperature and microturbulent velocity were determined by requiring a zero slope for the Fe abundance from Fe I lines as a function of the lower excitation potential of the line and as a function of the equivalent width of the line, respectively. The gravity was determined by requiring the mean Fe abundance derived from Fe I and Fe II lines to be the same. These steps were done iteratively until a solution satisfying the above conditions was found simultaneously for all three parameters. The results are $T_{\rm eff} = 4500 \pm 100$ K, $\log g = 2.3 \pm 0.2$, and $\xi = 1.8 \pm 0.1$ km s^{-1}. The errors in $T_{\rm eff}$ and ξ are based on 1 σ errors of the slopes described above. The error in $\log g$ is based on the 1 σ error of the mean Fe II abundance.

Analysis of the 1996 spectrum produced a best fit for $T_{\rm eff} = 4450 \pm 100$ K, $\log g = 2.2 \pm 0.2$, and $\xi = 1.9 \pm 0.1$ km s^{-1}. Given the uncertainties, the results are identical to those of the 1994 spectrum; in particular, there is no $T_{\rm eff}$ change in the atmosphere of HDE 233517. The average temperature, gravity, and microturbulent velocity derived from the two spectra (Table 3) were adopted in the subsequent analysis.

3.6. *Metallicities*

The large wavelength coverage in the echelle spectrum of HDE 233517 allowed us to determine two key metallicities.

The 49 Fe I lines measured in the 1994 spectrum gave an Fe abundance $[{\rm Fe/H}] = -0.36 \pm 0.03$, in agreement with seven Fe II lines, which gave $[{\rm Fe/H}] = -0.36 \pm 0.12$. Forty-six Fe I lines were measured in the 1996 spectrum. These gave an Fe abundance of $[{\rm Fe/H}] = -0.39 \pm 0.03$, and five Fe II lines gave $[{\rm Fe/H}] = -0.33 \pm 0.10$. Our mean values of the effective temperature, gravity, and Fe abundance of HDE 233517 corroborate Fekel et al.'s (1996) estimate that the spectrum of the star resembles α Ari (K2 III).

TABLE 3

ATMOSPHERIC PARAMETERS AND METALLICITY

Parameter	HDE 233517	HD 9746
$T_{\rm eff}$ (K)	4475 ± 100	4400 ± 150
$\log g$	2.25 ± 0.20	2.3 ± 0.2
ξ (km s^{-1}).....	1.85 ± 0.10	1.5 (assumed)
[Fe/H]	−0.37 ± 0.03	...
[Ca/H]	−0.32 ± 0.08:	...

The equivalent widths of eight Ca I lines were measured from the 1994 spectrum. Their oscillator strengths were derived from the solar spectrum with $\log \epsilon({\rm Ca/H}) = 6.36$. From these lines, the calcium abundance of HDE 233517 was determined to be $[{\rm Ca/H}] = -0.32 \pm 0.08$, $[{\rm Ca/Fe}] = 0.05 \pm 0.10$. We caution that many of the measured Ca I lines are very strong; only one line has an equivalent width of less than 100 mÅ, while the remaining equivalent widths range between 108 and 283 mÅ. Therefore, the calcium abundance may be somewhat more uncertain than this formal error. Table 3 lists the Ca abundance and the mean Fe abundance.

3.7. *Lithium*

3.7.1. *LTE Abundance Analysis*

The Li abundance in HDE 233517 was determined via spectral synthesis from both the Li I resonance line at 6707.8 Å and the excited line at 6103.6 Å. The major contribution to both these Li features comes from the more abundant ^{7}Li isotope. ^{7}Li has a significant big bang component, but the lighter, more fragile isotope, ^{6}Li, is formed principally by spallation reactions in cosmic rays. The current solar neighborhood ISM has a ^{7}Li/^{6}Li ratio of ≈ 10 (Lemoine, Ferlet, & Vidal-Madjar 1995), which is well matched by the meteoritic ratio of 12 (Anders & Grevesse 1989). In the absence of significant Li depletion, stellar Li I features contain contributions from both ^{7}Li and ^{6}Li components. Any depletion of ^{7}Li is expected to be accompanied by the complete destruction of ^{6}Li. We determined the ^{7}Li abundance of HDE 233517 under conditions of LTE in two ways: first, by assuming the ISM ratio of ^{7}Li/^{6}Li = 10 [hereafter referred to as Li(6+7)], which implies that no ^{7}Li destruction has occurred, and second, by assuming no contribution from ^{6}Li [hereafter referred to as Li(7)].

The Li I λ6707.8 resonance line consists of a doublet split by fine structure. The wavelengths of the components were taken from Meissner, Murdie, & Skelson (1948), and the oscillator strengths were adopted from the lifetime measurements of Gaupp, Kuske, & Andra (1982). The oscillator strengths of ^{6}Li were scaled to the ISM ^{7}Li/^{6}Li ratio of 10. The synthetic fit used $v \sin i = 17.6$ km s^{-1} and a 2 pixel Gaussian broadening of 0.2 Å. The Li abundance from the resonance line is $\log \epsilon(^7{\rm Li}) = 3.30 \pm 0.14$. The error results from an uncertainty of ± 0.10 dex in the fit, estimated by eye, combined with the errors in the model atmosphere parameters (mainly in $T_{\rm eff}$). The best fit to the 1996 spectrum yielded an Li abundance of $\log \epsilon(^7{\rm Li}) = 3.35 \pm 0.14$, nearly identical to the 1994 result. An overlay of the two spectral lines shows essentially no difference in their profiles. We adopt the mean abundance of $\log \epsilon(^7{\rm Li}) = 3.32 \pm 0.14$ for the Li(6+7) abundance from the resonance line. With no contribution from ^{6}Li, the Li I resonance line is best fitted with an Li abundance of $\log \epsilon(^7{\rm Li}) = 4.20 \pm 0.14$. The 1996 spectrum is best fitted with $\log \epsilon(^7{\rm Li}) = 4.25 \pm 0.14$ for a mean abundance of $\log \epsilon(^7{\rm Li}) = 4.22 \pm 0.14$.

In a previous analysis of HDE 233517, Fekel et al. (1996) determined a log Li abundance of 3.3. That value was obtained from an equivalent-width analysis of the Li I resonance line with curves of growth generated for dwarfs (Soderblom et al. 1993) and is therefore more uncertain.

TABLE 4

Li I Equivalent Widths from Spectral Synthesis

Wavelength (Å)	Equivalent Width (mÅ)		
	HDE 233517[a]	HDE 233517[b]	HD 9746
6707.8	528	546	455
6103.6	231	239	161

[a] From 1994 spectrum.
[b] From 1996 spectrum.

In most late-type giants with typical Li abundances, the λ6707.8 resonance line is the only measurable feature. In giants with large resonance-line equivalent widths, however, the Li I λ6103.6 excited feature can also be analyzed. The excited feature is on the wing of an Fe I line, which is at the red end of an Fe I, Ca I, Fe I, Fe I quartet. The wavelengths of the Fe I and Ca I features were taken from Moore, Minnaert, & Houtgast (1966), with those of the Fe I lines verified from the list of Nave et al. (1994). Oscillator strengths for the four lines were determined by forcing them to fit the solar spectrum with the standard solar abundances for Fe and Ca listed above. Since the Li I resonance feature at 6707.8 Å in the solar spectrum is itself minute, the excited feature has no significant contribution to the Fe I, Ca I, Fe I, Fe I quartet, and it was neglected in the fit. The ^{7}Li wavelengths and oscillator strengths are taken from the NIST Atomic Spectra database (Fuhr et al. 1999[2]). The ^{6}Li wavelengths were estimated from the resonance-line wavelengths by assuming $\Delta v/v$ = constant. As before, the ^{6}Li oscillator strengths were scaled to the ISM ^{7}Li/^{6}Li ratio of 10. With the ^{6}Li contribution, the abundance is $\log \epsilon(^7\mathrm{Li}) = 3.85 \pm 0.14$. Without ^{6}Li, the abundance is $\log \epsilon(^7\mathrm{Li}) = 4.00 \pm 0.14$, where the errors include errors in the model atmosphere parameters. The results are identical for the 1996 spectrum. Table 4 lists the equivalent widths of the Li I resonance and excited lines as determined from spectral syntheses of the 1994 and 1996 spectra. The various Li abundance results are summarized in Table 5.

We note several aspects of these results. All the Li abundance values equal or exceed the meteoritic value of $\log \epsilon(\mathrm{Li}) = 3.3$ (Anders & Grevesse 1989). The Li(7) abundances, derived from the resonance and excited features, are in close agreement within the errors, but the Li(6+7) abundances differ significantly. For each spectral feature, the difference between the Li(7) and Li(6+7) abundances is larger than the input ^{7}Li/^{6}Li ratio of 10. Although the difference is only slightly larger (0.15 dex) for the abundances from the excited line, the difference is much larger (0.90 dex) for the abundances from the resonance line, suggesting that saturation effects are involved. Note that the abundance errors listed in Table 5 include systematic and random errors. Both the resonance and excited line based abundances increase or decrease in the same direction when systematic errors come into play, and therefore the Li(6+7) abundance discrepancy is more significant than the total errors on the final values suggest.

[2] See http://physics.nist.gov/asd.

3.7.2. *Abundance Discrepancy*

The closer agreement between the Li(7) abundances measured from the resonance and excited features argues that all ^{6}Li has been destroyed in HDE 233517. This, coupled with the supermeteoritic value of the Li(7) abundance, has significant implications for the production of Li in Li-rich giants. Before we discuss these, we investigate possible explanations for the discrepant Li(6+7) abundances.

Is the Li I *excited line contaminated?* The large abundances yielded by this line lead to an immediate question: is it contaminated by a line that is weak and has negligible contribution in the solar spectrum, but becomes very strong in the low gravity of the giant leading to an overestimate of the Li I contribution by its exclusion from the synthesis? To check this, we analyzed a spectrum of Arcturus, obtained during the 1996 November KPNO observing run, using $T_{\rm eff} = 4300$ K, $\log g = 1.8$, [Fe/H] = -0.5, and [Ca/Fe] = $+0.3$ (Peterson, Dalle Ore, & Kurucz 1993) for the synthesis. Because both destruction and dilution lead to the extensive loss of Li in Arcturus, the Li I excited line does not contribute to the quartet feature. We found the observed line quartet to be well fit with the Fe I and Ca I lines alone, and there is no additional feature of the magnitude predicted by the abundance difference between the Li I(6+7) resonance and excited values. The simple explanation that the large excited-line abundance is in error is thus eliminated.

Is the Li I *resonance line too weak?* A decrease in the strength of the resonance line may be caused, for example, by chromospheric emission filling in the feature. HDE 233517 shows modest Ca II H and K emission (Fekel et al. 1996). To examine this possibility more closely, we compared the spectrum of HDE 233517 to that of Arcturus. The slightly lower temperature and metallicity of Arcturus combine to produce neutral metal lines whose strengths are identical to those of HDE 233517. We examined the Na I D lines and the K I resonance line to look for evidence of chromospheric filling in. Figure 3*a* shows the Na I D lines and Figure 3*b* the K I resonance line of HDE 233517 compared with the broadened spectrum of Arcturus. Note that the photospheric lines are well matched; the exceptions in the K I region are all telluric features. In particular, the

TABLE 5

log ^{7}Li Abundances

Star	Isotope	LTE		Non-LTE	
		λ6707.8	λ6103.6	λ6707.8	λ6103.6
HDE 233517.....	6+7	3.32 ± 0.14	3.85 ± 0.14	...	...
	7	4.22 ± 0.18	4.00 ± 0.14	4.22 ± 0.11	4.22 ± 0.11
HD 9746	6+7	3.00 ± 0.18	3.40 ± 0.18	...	...
	7	3.85 ± 0.18	3.50 ± 0.18	3.75 ± 0.16	3.75 ± 0.16

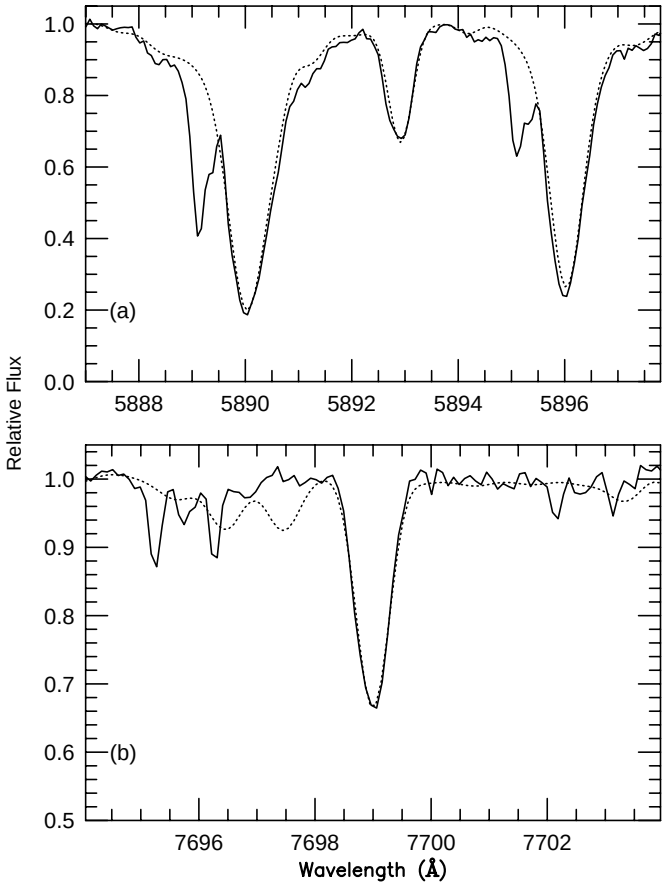

FIG. 3.—(*a*) Na D lines from the 1994 spectrum (*solid line*) of HDE 233517 compared with a rotationally broadened spectrum of Arcturus (*dotted line*). Blueshifted components not matched by the Arcturus spectrum are interstellar features. (*b*) The K I resonance feature (7699.0 Å) of HDE 233517 (*solid line*) compared with a rotationally broadened spectrum of Arcturus (*dotted line*). The mismatched broadened lines are telluric features in the Arcturus spectrum.

Na I D lines and the K I resonance line are not significantly weaker in HDE 233517. A more thorough analysis of alkali-element line formation may be required to investigate this point further.

It is also possible that the stellar atmosphere is more extended, by mass loss for example, and not adequately represented by the standard model atmosphere used in this analysis. If one truncates the current model atmosphere further, say, reducing the number of levels so that the optical depth in the outer layers is reduced from 10^{-7} to 10^{-4}, the abundance derived from the resonance line decreases far more than the excited-line abundance. By inference, if the model atmosphere were more extended, the abundance derived from the resonance line would be larger. Quantitative estimates would require such a model atmosphere.

While it is possible that the Li(6+7) abundance discrepancy between the resonance and excited lines is due to the nonstandard atmosphere of HDE 233517, we have found no simple manifestation of such a phenomenon in our examination of other alkali-element lines. We argue, therefore, that the discrepancy in the Li(6+7) abundance is most likely due to saturation effects. The ^{7}Li resonance line is strong and saturated. Introducing a ^{6}Li component with a tenth of the abundance desaturates the resonance line and produces an abundance that is significantly smaller than the unsaturated excited line.

3.7.3. *Non-LTE*

To determine the influence of departures from LTE on the Li abundance determination in HDE 233517, we solved radiative transfer and statistical equilibrium equations for all relevant wavelengths and levels in Li I with the same model atmospheres that were used in the LTE analysis. We employed the Multilevel Accelerated Lambda Iteration (MALI) technique of Rybicki & Hummer (1991, 1992) as coded by Uitenbroek in the computer programs RHF1D and RHSPHERE for plane-parallel and spherical geometry, respectively. The model of the lithium atom was the same as that used by Uitenbroek (1998) to investigate the influence of photospheric granulation on the determination of Li abundances in solar-type stars. It is complete to quantum number $n = 3$ and has nine levels and 11 lines with explicit fine structure. Although radiative ionization from all neutral Li levels was solved for explicitly, the effect of line blanketing due to metallic UV lines on ionization rates was not taken into account. In reality, this blanketing reduces radiative ionization rates, leaving more atoms in the neutral stage and slightly increasing opacity and deepening the lines (see Carlsson et al. 1994). A test calculation, where the UV line blanketing was mimicked by a multiplicative factor (the magnitude of which was determined by requiring a solar model to match the observed solar flux) to the background opacity due to bound-free transitions, electron scattering, and other opacity sources, showed that omitting the blanketing opacity may lead to an overestimate of the lithium abundance by 0.1–0.2 dex.

For HDE 233517 $\log g = 2.25$, which translates into an atmospheric extent of about 1% of the stellar radius, enough to warrant the inclusion of spherical geometry effects in a non-LTE transfer solution. The spherical geometry provides the radiation field with a larger solid angle for photon losses resulting in enhanced non-LTE effects compared to the plane-parallel solution. Most notably, the line source functions of both the Li resonance line and excited line are reduced, resulting in slightly deeper lines and lower determined abundances. In addition, limb darkening is enhanced by spherical geometry. This has little effect on the computed flux, which is heavily weighted toward the large projected area of the stellar disk center, but it has a more pronounced effect on the rotational broadening of the computed profile because of the rapid rotation of HDE 233517. Line broadening is weighted more to the larger projected line-of-sight velocity at the limb of the star. Including spherical geometry improved the fit of the Li λ6103.6 line and the blueward Fe I–Ca I quartet appreciably.

With our spherical non-LTE calculations, we obtained good fits to both lines (Figs. 4*a* and 4*b*) with a single abundance value, $\log \epsilon(^7\mathrm{Li}) = 4.22 \pm 0.05$, without introducing a contribution from ^{6}Li. Factoring in the uncertainties in the model atmosphere parameters results in a more conservative estimate of $\log \epsilon(^7\mathrm{Li}) = 4.22 \pm 0.11$ (Table 5). We also find that in the applicable abundance regime of $\log \epsilon(^7\mathrm{Li}) \approx 4$, which is slightly beyond the abundances covered by the calculation of Carlsson et al. (1994), the excited Li line at 6103.6 Å in our non-LTE calculations is more sensitive to abundance variations than the resonance line at 6707.8 Å. This is because the excited line forms nearly

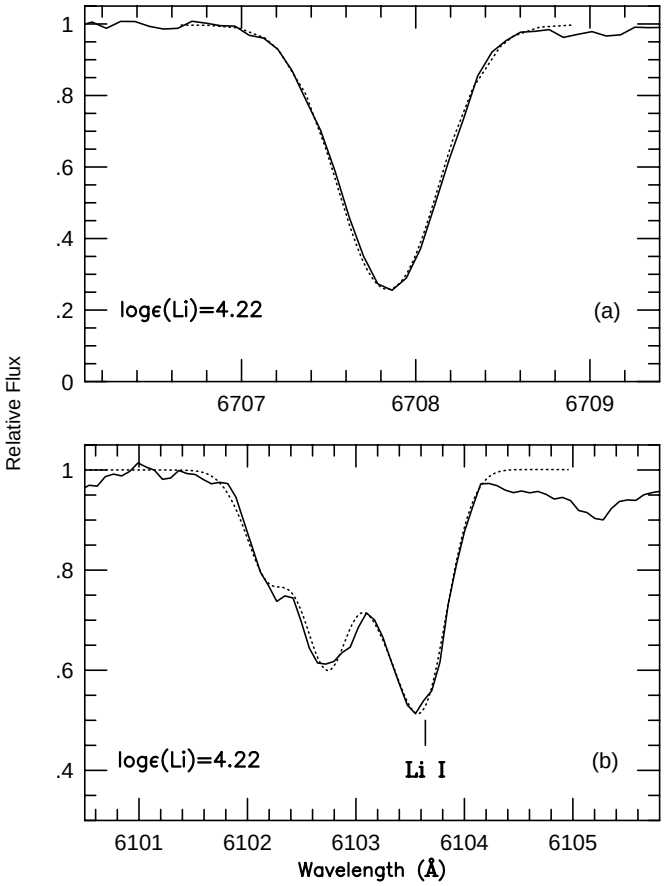

FIG. 4.—Li I (*a*) λ6707.8 resonance and (*b*) λ6103.6 excited lines of HDE 233517 (*solid lines*) are shown together with the synthetic fits (*dotted lines*) calculated with the effects of spherical geometry under non-LTE conditions.

in LTE on the steeper part of the Planck function so a small variation in opacity results in considerable line-core intensity variation. The resonance line, on the other hand, forms in a region where its source function is almost flat due to scattering in the line itself, making the line depth much less sensitive to abundance variations.

Although we did not calculate non-LTE Li(6+7) abundances, we note that given the direction and magnitude of the non-LTE corrections (Carlsson et al. 1994), this will serve to increase the already significant discrepancy between the excited and resonance line based abundances.

4. HD 9746: ANALYSIS AND RESULTS

In light of our findings for HDE 233517, we have reexamined our previous result for the Li-rich giant HD 9746 (Fekel & Balachandran 1993), whose basic observational properties are listed in Table 1. With $T_{\rm eff} = 4400$ K and $\log g = 3.0$, our earlier Li(6+7) analysis of the Li I resonance line yielded $\log \epsilon(\mathrm{Li}) = 2.8$.

4.1. *Atmospheric Parameters*

The $T_{\rm eff} = 4400$ K from Fekel & Balachandran (1993) was retained. This is in good agreement with the value of 4420 K derived by Brown et al. (1989). The previously adopted gravity of HD 9746 was an estimate based on its luminosity class (Fekel & Balachandran 1993). Here we have computed a more precise value of $\log g = 2.3 \pm 0.2$ dex from an assumed mass of 2.0 $M_\odot$ and the *Hipparcos* parallax of 0.″00777 ± 0.″00082 (Perryman et al. 1997). The microturbulent velocity was assumed to be 1.5 km s^{-1}.

4.2. *Lithium*

With the revised model atmosphere parameters, the earlier Li I λ6707.8 resonance-line spectrum and the newly acquired KPNO coudé spectrum of the Li I λ6103.6 excited line were reanalyzed with and without ^{6}Li under conditions of both LTE and non-LTE. Under LTE, when ^{6}Li is included in the analysis, the resulting abundances are $\log \epsilon(^7\mathrm{Li}) = 3.00 \pm 0.18$ and 3.40 ± 0.18 from the resonance and excited lines, respectively. Analysis of the resonance feature with ^{7}Li alone alters the abundance value to $\log \epsilon(\mathrm{Li}) = 3.85 \pm 0.18$ and the excited-line result, in better agreement, to $\log \epsilon(\mathrm{Li}) = 3.50 \pm 0.18$. These results are listed in Table 5.

The non-LTE analysis of both features followed the same procedure outlined in § 3.7.3. While $\log g = 2.3$ for HD 9746 is the same as that of HDE 233517, because of its smaller $v \sin i$ value of 9 km s^{-1}, spherical geometry had a smaller effect on the abundance derived from the Li I excited line of HD 9746. Both Li I lines were fitted with $\log \epsilon(^7\mathrm{Li}) = 3.75 \pm 0.05$ (Figs. 5*a* and 5*b*). Factoring in the errors due to the uncertainties in the model atmosphere parameters results in a more conservative estimate of $\log \epsilon(^7\mathrm{Li}) = 3.75 \pm 0.16$ (Table 5). Table 4 lists the equivalent width of the Li I resonance and excited lines as derived

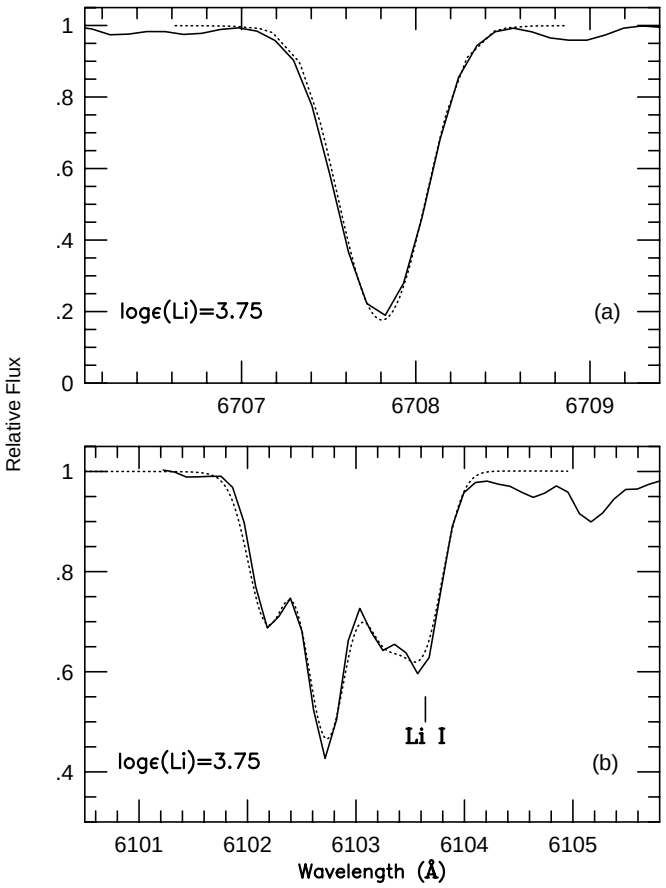

FIG. 5.—Li I (*a*) λ6707.8 resonance and (*b*) λ6103.6 excited lines of HD 9746 (*solid lines*) are shown together with the synthetic fits (*dotted lines*) calculated with the effects of spherical geometry under non-LTE conditions.

from the spectral synthesis. As for HDE 233517, we note that non-LTE corrections to the Li(6+7) abundance (Carlsson et al. 1994) will serve to increase the difference between the resonance- and excited-line abundances.

Pavlenko, Savanov, & Yakovina (1999) have recently carried out both LTE and non-LTE analyses of the Li I lines in HD 9746. Their atmospheric parameters of $T_{\rm eff} = 4420$, $\log g = 2.3$, and $\xi = 1.4$ km s^{-1} are in good agreement with ours. They do not include ^{6}Li in their analyses. Their final non-LTE result of $\log \epsilon(\mathrm{Li}) = 3.65$ is in reasonable agreement with our result of 3.75. However, their LTE resonance-line abundance is 0.15 dex larger than ours, and their non-LTE correction of 0.4 dex for the resonance line is twice as large as ours. Pavlenko & Magazzu (1996) plot differences between the non-LTE abundance corrections computed by them and by Carlsson et al. (1994) for dwarfs, which are typically of order 0.1 dex. The difference between our results and those of Pavlenko et al. are probably due to slight differences in the atmospheric and atomic models used. For example, we used a mixing length of $L/H = 1.25$, whereas Pavlenko et al. used 1.5. This affects the steepness of the temperature gradient deep in the atmosphere, which in turn determines the amount of non-LTE overionization of lithium.

5. DISCUSSION

5.1. *Evolutionary Status*

Although the lack of a *Hipparcos* parallax (Perryman et al. 1997) for HDE 233517 precludes a determination of its luminosity, we can compute a minimum value. As with other chromospherically active stars, the photometric variability of HDE 233517 results from star spots in a nonuniform distribution that rotate in and out of view. Thus, we adopt the mean photometric period as the rotation period of the star. The rotation period of 47.9 ± 0.6 days and $v \sin i = 17.6 \pm 1.0$ km s^{-1} result in $R \sin i = 16.7 \pm 1.0$ $R_\odot$. This value, combined with our mean $T_{\rm eff} = 4475 \pm 100$ K, produces a minimum luminosity of 100 ± 14 $L_\odot$. Comparison with the models of Palla & Stahler (1990) indicates that this minimum luminosity for HDE 233517 is a factor of 10 above the stellar birth line, ruling out a pre–main-sequence status. Our $T_{\rm eff}$ and the relations of Flower (1996) produce a minimum $M_v = 0.37 \pm 0.19$ mag and a minimum distance of 617 ± 80 pc. The latter is consistent with the value estimated from its spectral type by Fekel et al. (1996).

The *Hipparcos* parallax (Perryman et al. 1997) and the assumption of no ISM reddening for HD 9746 produce $M_V = 0.37 \pm 0.23$ mag. Adopting the bolometric correction from Flower (1996) results in $L = 87 \pm 20$ $L_\odot$, which with the adopted $T_{\rm eff} = 4400 \pm 150$ K produces a radius of 16.1 ± 2.2 $R_\odot$. These parameters are nearly identical to the minimum values calculated for HDE 233517. The position of HD 9746 on the H-R diagram and its ^{12}C/^{13}C ratio of 28 ± 4 (Brown et al. 1989) clearly identify it as a post–main-sequence giant.

The derived properties for both giants are listed in Table 6.

TABLE 6

DERIVED PROPERTIES

Parameter	HDE 233517[a]	HD 9746[b]
R ($R_\odot$)	$>16.7 \pm 1.0$	16.1 ± 2.2
L ($L_\odot$)	$>100 \pm 14$	87 ± 20
M_v (mag).....	$<0.36 \pm 0.19$	0.37 ± 0.23
d (pc)	$>617 \pm 80$	129 ± 13

[a] Minimum values derived from $v \sin i$ and $P_{\rm rot}$.
[b] Values derived from *Hipparcos* parallax.

5.2. *Other Supermeteoritic Li-rich Giants?*

Of all the first-ascent Li-rich stars that have been discovered so far (see Charbonnel & Balachandran 2000 for a compilation), HDE 233517 has the largest Li abundance. A comparable value has been claimed for HD 19745 by de la Reza & da Silva (1995), but their analysis is highly uncertain. The effective temperature of HD 19745 was obtained merely by remarking on the spectral similarity with the Hyades giant γ Tau. The LTE abundance from the λ6707.8 line is not listed, as the authors were unable to simultaneously fit the wings and core of the Li I resonance line, a problem we do not encounter in HDE 233517. Although γ Tau is a metal-rich Hyades giant, de la Reza & da Silva (1995) adopted a metallicity of $[\mathrm{Fe/H}] = -0.05$, which they used to determine the oscillator strengths of the Fe I, Ca I, Fe I, Fe I quartet blueward of the Li I λ6103.6 excited line. These oscillator strengths were then used in the subsequent analysis of HD 19745. Given the effective temperature and oscillator strength uncertainties, the LTE Li abundance of $\log \epsilon(\mathrm{Li}) = 4.08$ obtained from the λ6103.6 excited line is probably far more uncertain than the 0.1 dex error stated by the authors. Their non-LTE analysis adds further confusion. The non-LTE abundance required to match the profiles of both the excited and resonance Li I lines in HD 19745 is listed as $\log \epsilon(\mathrm{Li}) = 4.75$ by the authors, resulting in a non-LTE correction of +0.67 dex for the λ6103 excited feature. This is not corroborated by Carlsson et al.'s (1994) calculations, from which a correction of +0.1 dex may be computed. The Li I excited feature does indeed appear to be very strong in the spectrum of HD 19745 (Fig. 4 of de la Reza & da Silva 1995), but, in the final analysis, the published abundance is highly uncertain. The Li abundance of HDE 233517, therefore, remains uniquely high among first-ascent Li-rich giants.

5.3. *Origin of the Lithium Excess*

In HDE 233517 and HD 9746 we have demonstrated that the ^{7}Li abundances from the resonance and excited Li I lines are in better agreement when ^{6}Li is excluded from the spectral synthesis, suggesting that ^{7}Li has been freshly synthesized in the stellar interior. Further evidence for ^{7}Li production comes from Castilho et al.'s (1999) study, which suggests that normal dilution of Be has occurred in two Li-rich giants, HD 146850 and HD 787. Another study of Be, based on *IUE* data, was carried out in two other Li-rich giants, HD 9746 and HD 112127 (de Medeiros et al. 1997). The authors claimed that there is no sign of significant Be II features in these giants, indicating that Be dilution has occurred, but the results are more uncertain. Additional studies of Be abundances in Li-rich giants would be most useful.

Charbonnel & Balachandran (2000) have recently compiled a list of Li-rich giants from the literature. Using *Hipparcos* parallaxes, they calculated the luminosities of the stars and derived their masses from evolutionary tracks. An important result of this exercise was their finding that not all the stars that have previously been classified as Li-rich

are truly so; of the 20 Li-rich stars in their list, eight are either in the process of undergoing dilution or have completed a normal level of Li dilution and are thus Li-normal. Based on their positions on the H-R diagram and the internal structure of stars at those stages of evolution, Charbonnel & Balachandran (2000) hypothesized that Li is produced at two evolutionary phases on the red giant branch, which coincide with the close proximity of the surface convection zone to the hydrogen-burning shell. In low-mass stars (i.e., those that later undergo the helium flash), the first episode occurs during the red giant bump phase when the hydrogen-burning shell advances through the mean molecular weight gradient left behind by the first dredge-up. Once this barrier is erased, an as yet unidentified mixing process bridges the gap between the base of the convective zone and the hydrogen-burning shell. Material in the ^{3}He-rich envelope is subjected to temperatures high enough to convert ^{3}He into ^{7}Be via the Cameron-Fowler (1971) process: ^{3}He(α,γ)^{7}Be. The freshly synthesized ^{7}Be is rapidly transported to cooler regions where it subsequently decays into ^{7}Li via ^{7}Be(e^-,ν)^{7}Li. In intermediate-mass stars, which do not undergo the helium shell flash, the mean molecular weight gradient is not erased until the star is burning He in its core, i.e., until the star is a clump giant. Therefore, mixing leading to ^{7}Li production does not occur during the first-ascent red giant phase but instead during the early–asymptotic giant branch (AGB) phase when the convective envelope deepens in response to core He exhaustion. Low-mass stars may also go through a second episode of Li enrichment at this phase.

The nonstandard or "extra" mixing required to produce the connection between the convection zone and the hydrogen-burning shell is not mandated by the Li observations alone. Rather, it was first postulated to explain the marked decrease in ^{12}C/^{13}C ratio in first-ascent red giants to values below those predicted by the standard models due to first dredge-up (e.g., Sweigart & Mengel 1979). Li production is the first step in this mixing process; CN cycle processing, which produces the observed decrease in the carbon-isotope ratio, follows as a result of deeper mixing. The latter is observed to have occurred in 96% of all low-mass field giants that have evolved past the red giant bump (Charbonnel & do Nascimento 1998). Such mixing is therefore ubiquitous. Charbonnel & Balachandran (2000) pointed out that once the convection zone material is mixed deep enough to undergo CN processing in the hydrogen-burning shell, the temperature is too high for ^{7}Li to survive, and, hence, the Li-rich phase must be short.

HDE 233517 and HD 9746 provide very strong support for the hypothesis of Charbonnel & Balachandran (2000). Although there is no *Hipparcos* parallax for HDE 233517, our luminosity estimate of $\geq 100\,L_\odot$ puts it at the red giant bump. From its *Hipparcos* luminosity estimate and a comparison with evolutionary tracks, the position of HD 9746 on the H-R diagram is in close proximity to that of HDE 233517. The extreme Li abundances of HDE 233517 and HD 9746 demonstrate that Li production has occurred at or prior to this phase. Two other Li-rich giants, HD 219025 and the lower mass ($1.1\,M_\odot$) star HD 112127, are members of this clump. According to the hypothesis of Charbonnel & Balachandran (2000), peak ^{7}Li values are not expected to accompany low ^{12}C/^{13}C ratios, and, indeed, this is consistent with the observations known to date. With standard ^{12}C/^{13}C ratios of 28 ± 4 (Brown et al. 1989) and 22 ± 7 (Wallerstein & Sneden 1982), respectively, HD 9746 and HD 112127 [$\log \epsilon(\mathrm{Li}) = 2.7$] have not yet undergone the deeper mixing that will trigger the CN cycle and lower the carbon-isotope ratios to nonstandard values. However, with masses comparable to HD 9746 and HDE 233517 and residing in the same Li-rich clump, HD 148293 and HD 183492 have lower carbon-isotope ratios of 16 and 9, respectively (Berdyugina & Savanov 1994), and lower Li abundances of $\log \epsilon(\mathrm{Li}) = 2.0$ (Brown et al. 1989). This is consistent with the hypothesis that CN processing has begun in these giants leading to a decline in Li from a possible peak value of 1–2 dex higher.

The hypothesis of Charbonnel & Balachandran (2000) appears to have identified with some certainty the first-ascent evolutionary phase where Li-rich giants form. However, the number of giants found so far in this evolutionary stage is quite small. Identification of additional cool giants with $\log \epsilon(\mathrm{Li}) \geq 2.0$ and determination of their ^{12}C/^{13}C ratios may impose additional constraints on the hypothesis and any proposed mixing mechanism. A measurement of the carbon-isotope ratio of HDE 233517 would be most useful.

5.4. *Clues to Understanding the Mixing Process*

The driver behind the extra-mixing process continues to remain enigmatic.

Rotational mixing has long been cited as a likely candidate (Sweigart & Mengel 1979). A connection with rapid rotation and chromospheric activity was made by Fekel & Balachandran (1993). Although most red giants are slow rotators, rapid rotation has been seen in a few isolated single stars, FK Comae being the most well-known example. Simon & Drake (1989) suggested that the rapid rotation observed on the surfaces of these stars may originate when the surface convective envelope deepens and dredges up angular momentum from an internal reservoir. The transfer of angular momentum creates a dynamo that results in chromospheric activity. Following up on this, Fekel & Balachandran (1993) measured Li abundances in a number of chromospherically active single giants and found many of them to have high Li abundances. Hence, they suggested that the dredge-up of angular momentum was accompanied by the dredge-up of ^{7}Be-rich material. It must be noted, however, that the spin-up of the surface of a red giant requires a vast reservoir of angular momentum. In the only star that has been probed in some detail, the Sun, helioseismology has not detected such a reservoir (Tomczyk, Schou, & Thompson 1995; Charbonneau et al. 1998). Fekel & Balachandran (1993) pointed out that a one-to-one correlation between high Li abundances, rapid rotation, and chromospheric activity would not be expected, since the timescales for enhancement and depletion of Li are not necessarily the same as the timescales for rotational spin-up and spin-down, or for increased or decreased Ca II H and K emission. There is also no direct correlation between the strength of chromospheric activity and the magnitude of the Li abundance. For example, HD 9746 has by far the stronger level of chromospheric activity, but its Li abundance is significantly smaller than HDE 233517.

De la Reza, Drake, & da Silva (1996) and de la Reza et al. (1997) have argued that Li enrichment is accompanied by mass loss. Their claim is based on the distribution of Li-rich giants in an IRAS color-color plot. They found that many

Li-rich giants show excess in the $25-12$ μm color and particularly in the $60-25$ μm color. HDE 233517 does indeed have excesses in both IRAS colors, and the unusual Hα profile (Fekel et al. 1996) provides evidence for mass loss. The changes seen in the Hα and Na D line profiles (Fig. 2) are indicative of variations in the mass-loss rate of the star. In the differenced Na D spectrum, the double-peaked profile with velocities of -25 and $+3$ km s^{-1} suggests at least two episodes of mass loss. With a velocity of -25 km s^{-1} the more recent episode is much more energetic than predicted by de la Reza et al.'s (1996) model. We note that, although there appear to be changes in the mass-loss rate of HDE 233517 between 1994 and 1996, there is no change in its Li content or its rotational velocity.

Although de la Reza et al. (1996, 1997) claimed that all stars between 1 and 2.5 $M_{\odot}$ undergo such mass loss and Li enrichment, they present no evidence for this sweeping claim. Following de la Reza et al.'s suggestions, Fekel & Watson (1998) and Jasniewicz et al. (1999) independently examined a number of infrared-excess stars but found no new Li-rich giants. Furthermore, Charbonnel & Balachandran (2000) have concluded that giants such as HD 108471, HD 120602, and HD 31993, which have an infrared excess and were previously characterized as Li-rich, are in fact Li-normal giants. Although some Li-rich stars certainly have infrared excesses, clearly there is no one-to-one correspondence between present Li excess and mass loss.

There is little disagreement among the various studies that, if ^{7}Li is indeed manufactured in the Li-rich giants as our results argue, it must occur by the Cameron-Fowler (1971) process. Following the hot-bottom convective-envelope model for Li production in the higher mass AGB stars (Sackmann & Boothroyd 1992), Sackmann & Boothroyd (1999) have suggested an ad hoc two-stream "conveyer belt" circulation model to transport material created via the Cameron-Fowler (1971) process from the vicinity of the hydrogen-burning shell to the convection zone in first-ascent red giants. By controlling the ascending and descending streams, the model is able to produce surface Li abundances as large as $\log \epsilon(\mathrm{Li}) = 4.0$ when mixing is continuous along the red giant branch. Given Charbonnel & Balachandran's (2000) finding that ^{7}Li production is not continuous but rather occurs at discrete evolutionary phases on the red giant branch, it appears that the observed behavior is better simulated by a short-lived mixing episode under the assumption of a particularly fast stream in Sackmann & Boothroyd's (1999) models. While Sackmann & Boothroyd's (1999) model may explain the logistics of Li production, it does not identify or explain the driving mechanism.

A possible alternative to a giant's internal Li production is the accretion of a planet's Li-rich material by an expanding red giant envelope (Alexander 1967; Brown et al. 1989). Since the discovery of short-period planets around solar-like stars (e.g., Mayor & Queloz 1995), there has been a more extensive presentation and analysis of this mechanism (Siess & Livio 1999). The accumulated observational evidence, however, now makes it abundantly clear that this process cannot viably explain the Li-rich giants. The accretion of a planet would result in the simultaneous enhancement of ^{6}Li, ^{7}Li, and Be. The lack of ^{6}Li in the spectra of HDE 233517 and HD 9746 and the lack of Be enrichment suggested in four other Li-rich giants is strong evidence against this scenario. Furthermore, it is difficult to produce the large Li abundances seen in HDE 233517 and HD 9746 by ingesting planets with meteoritic Li compositions. Acknowledging this fact, Siess & Livio (1999) suggest that planet ingestion may trigger mixing leading to ^{7}Li production by the Cameron-Fowler (1971) process. This gives planet ingestion only an incidental role in the formation of very Li-rich giants. Finally, there is no particular reason why planetary accretion should have taken place preferentially at the two clumps on the H-R diagram where Charbonnel & Balachandran (2000) have found all the Li-rich giants to be located. The Li evidence therefore suggests that, at best, the formation of an Li-rich giant by the accretion of a planet is very rare indeed.

6. CONCLUSIONS

The post–main-sequence stars HDE 233517 and HD 9746 have supermeteoritic ^{7}Li abundances. By the inclusion and exclusion of ^{6}Li in the syntheses, we have shown that consistent ^{7}Li abundances are obtained only when ^{6}Li is absent in the stellar atmosphere. This provides evidence for fresh ^{7}Li synthesis and excludes both preservation of primordial Li and planetary accretion as viable scenarios for the formation of Li-rich giants.

Although the mixing process remains enigmatic, we suggest that rapid rotation, excess chromospheric activity, and mass loss may all be symptoms that are triggered by the same process that leads to Li enrichment. The difference of 0.5 dex in Li between HDE 233517 and HD 9746 suggests that the efficiency of the mixing process may differ from star to star, but the statistics are currently too poor to provide meaningful constraints for models.

We hope that the additional clues we have unearthed in the Li-rich giants HDE 233517 and HD 9746 will provide further constraints on mixing models that seek to explain the production of ^{7}Li in giants.

S. C. B. is pleased to acknowledge support from NSF grants AST 96-18335 and AST 98-19870. This research has been supported in part by NASA grants NCC5-96 and NCC5-228 (which fund Tennessee State University's Center for Automated Space Science) and NSF grant HRD-9706268 (which funds TSU's Center for Systems Science Research).

REFERENCES

Anders, E., & Grevesse, N. 1989, Geochim. Cosmochim. Acta, 53, 197
Alexander, J. B. 1967, Observatory, 87, 238
Berdyugina, S. V., & Savanov, I. S. 1994, Astron. Lett., 20, 639
Brown, J. A., Sneden, C., Lambert, D. L., & Dutchover, E. 1989, ApJS, 71, 293
Cameron, A. G. W., & Fowler, W. A. 1971, ApJ, 164, 111
Carlsson, M., Rutten, R. J., Bruls, J. H. M. J., & Shchukina, N. G. 1994, A&A, 288, 860
Castilho, B. V., Spite, F., Barbuy, B., Spite, M., de Medeiros, J. R., & Gregorio-Hetem, J. 1999, A&A, 345, 249
Charbonneau, P., Tomczyk, S., Schou, J., & Thompson, M. J. 1998, ApJ, 496, 1015
Charbonnel, C., & Balachandran, S. C. 2000, A&A, 359, 563
Charbonnel, C., & do Nascimento, J. D., Jr. 1998, A&A, 336, 915
de la Reza, R., & da Silva, L. 1995, ApJ, 439, 917
de la Reza, R., Drake, N. A., & da Silva, L. 1996, ApJ, 456, L115
de la Reza, R., Drake, N. A., da Silva, L., Torres, C. A. O., & Martin, E. L. 1997, ApJ, 482, L77
de Medeiros, J. R., Lèbre, A., de Garcia Maia, M. R., & Monier, R. 1997, A&A, 321, L37

Eaton, J. A. 1995, AJ, 109, 1797
Fekel, F. C. 1997, PASP, 109, 514
Fekel, F. C., & Balachandran, S. 1993, ApJ, 403, 708
Fekel, F. C., & Watson, L. C. 1998, AJ, 116, 2466
Fekel, F. C., Webb, R. A., White, R. J., & Zuckerman, B. 1996, ApJ, 462, L95
Fitzpatrick, M. J. 1993, in ASP Conf. Ser. 52, Astronomical Data Analysis Software and Systems II, ed. R. J. Hanish, R. V. J. Brissenden, & J. Barnes (San Francisco: ASP), 472
Flower, P. J. 1996, ApJ, 469, 355
Fuhr, J. R., et al. 1999, Atomic Spectra Database v2.0 (Washington, DC: Natl. Inst. Standards Tech.)
Gaupp, A., Kuske, P., & Andra, H. J. 1982, Phys. Rev. A, 26, 3351
Gratton, R. G., & D'Antona, F. 1989, A&A, 215, 66
Henry, G. W. 1995a, in ASP Conf. Ser. 79, Robotic Telescopes: Current Capabilities, Present Developments, and Future Prospects for Automated Astronomy, ed. G. W. Henry & J. A. Eaton (San Francisco: ASP), 44
———. 1995b, in ASP Conf. Ser. 79, Robotic Telescopes: Current Capabilities, Present Developments, and Future Prospects for Automated Astronomy, ed. G. W. Henry & J. A. Eaton (San Francisco: ASP), 37
———. 1996, in ASP Conf. Ser. 87, New Observing Modes for the Next Century, ed. T. Boroson, J. Davies, & I. Robson (San Francisco: ASP), 145
Hobbs, L. M. 1974, ApJ, 191, 381
Jasniewicz, G., Parthasarathy, M., de Laverny, P., & Thevenin, F. 1999, A&A, 342, 831
Kurucz, R. L., Furenlid, I., Brault, J., & Testerman, L. 1984, Solar Flux Atlas from 296 to 1300 nm (Cambridge: Office Univ. Publ.)
Lemoine, M., Ferlet, R., & Vidal-Madjar, A. 1995, A&A, 298, 879
Mallik, S. 1993, ApJ, 402, 303
Mayor, M., & Queloz, D. 1995, Nature, 378, 355
Meissner, K. W., Murdie, L. G., & Skelson, P. H. 1948, Phys. Rev., 74, 932
Miroshnichenko, A. S., Bergner, Yu. K., & Kuratov, K. S. 1996, A&A, 312, 521
Moore, C. E., Minnaert, M. G. J., & Houtgast, J. 1966, The Solar Spectrum 2935 Å to 8770 Å (NBS Monogr. 61; Washington, DC: US Gov. Printing Office)
Nave, G., Johansson, S., Learner, R. C. M., Thorne, A. P., & Brault, J. W. 1994, ApJS, 94, 221
Nicolet, B. 1978, A&AS, 34, 1
Palla, F., & Stahler, S. W. 1990, ApJ, 360, L47
Pavlenko, Ya. V., & Magazzu, A. 1996, A&A, 311, 961
Pavlenko, Ya. V., Savanov, I. S., & Yakovina, L. A. 1999, Astron. Rep., 43, 671
Perryman, M. A. C., et al. 1997, The *Hipparcos* and Tycho Catalogues (ESA-SP 1200; Noordwijk: ESA)
Peterson, R. C., Dalle Ore, C. M., & Kurucz, R. L. 1993, ApJ, 404, 333
Pilachowski, C. A., Sneden, C., & Hudek, D. 1990, AJ, 99, 1225
Rybicki, G. B., & Hummer, D. G. 1991, A&A, 245, 171
———. 1992, A&A, 262, 209
Sackmann, I.-J., & Boothroyd, A. I. 1992, ApJ, 392, L71
———. 1999, ApJ, 510, 217
Scarfe, C. D., Batten, A. H., & Fletcher, J. M. 1990, Publ. Dom. Astrophys. Obs. Victoria, 18, 21
Siess, L., & Livio, M. 1999, MNRAS, 308, 1133
Simon, T., & Drake, S. A. 1989, ApJ, 346, 303
Skinner, C. J., et al. 1995, ApJ, 444, 861
Sneden, C. 1973, Ph.D. thesis, Univ. Texas
Soderblom, D. R., Jones, B. F., Balachandran, S., Stauffer, J. R., Duncan, D. K., Fedele, S. B., & Hudon, J. D. 1993, AJ, 106, 1059
Strassmeier, K. G., & Hall, D. S. 1988, ApJS, 67, 453
Sweigart, A. V., & Mengel, J. G. 1979, ApJ, 229, 624
Tomczyk, S., Schou, J., & Thompson, M. J. 1995, ApJ, 448, L57
Uitenbroek, H. 1998, ApJ, 498, 427
Walker, H. J., & Wolstencroft, R. D. 1988, PASP, 100, 1509
Wallerstein, G., & Sneden, C. 1982, ApJ, 255, 577